Chin. Geogra. Sci. 2013 Vol. 23 No. 2 pp. 131–146
doi: 10.1007/s11769-013-0596-7

Springer Science Press
www.springerlink.com/content/1002-0063

Comparison Between Reconstructions of Global Anthropogenic Land Cover Change over Past Two Millennia

YAN Mi[1, 2], WANG Zhiyuan[2, 3], Jed Oliver KAPLAN[4], LIU Jian[1, 2], MIN Shen[2], WANG Sumin[2]

(1. *Key Laboratory of Virtual Geographic Environment of Ministry of Education*, *School of Geography Science*, *Nanjing Normal University*, *Nanjing* 210046, *China*; 2. *State Key Laboratory of Lake Science and Environment*, *Nanjing Institute of Geography and Limnology*, *Chinese Academy of Sciences*, *Nanjing* 210008, *China*; 3. *University of Chinese Academy of Science*, *Beijing* 100049, *China*; 4. *Environmental Engineering Institute*, *Ecole Polytechnique Fédérale de Lausanne*, *Station* 2, 1015 *Lausanne*, *Switzerland*)

Abstract: Three global datasets, the History Database of the Global Environment (HYDE), Kaplan and Krumhardt (KK) and Pongratz of reconstructed anthropogenic land cover change (ALCC) were introduced and compared in this paper. The HYDE dataset was reconstructed by Goldewijk and his colleagues at the National Institute of Public Health and the Environment in Netherland, covering the past 12 000 years. The KK dataset was reconstructed by Kaplan and his colleagues, the Soil-Vegetation-Atmosphere Research Group at the Institute of Environmental Engineering in Switzerland, covering the past 8000 years. The Pongratz dataset was reconstructed by Pongratz and her colleagues at the Max Planck Institute for Meteorology in Germany, covering AD 800–1992. The results show that the reconstructed datasets are quite different from each other due to the different methods used. The three datasets all allocated the historical ALCC according to human population density. The main reason causing the differences among the three datasets lies on the different relationships between population density and land use used in each reconstructed dataset. The KK dataset is better than the other two datasets for two important reasons. First, it used the nonlinear relationship between population density and land use, while the other two used the linear relationship. Second, Kaplan and his colleagues adopted the technological development and intensification parameters and considered the wood harvesting and the long-term fallow area resulted from shifting cultivation, which were neglected in the reconstructions of the other two datasets. Therefore, the KK dataset is more suitable as one of the anthropogenic forcing fields for climate simulation over the past two millennia that is recently concerned by two projects, the National Basic Research Program and the Strategic and Special Frontier Project of Science and Technology of the Chinese Academy of Sciences.

Keywords: anthropogenic land cover change (ALCC); spatial pattern; vegetation type; global dataset; last two millennia

Citation: Yan Mi, Wang Zhiyuan, Kaplan Jed Oliver, Liu Jian, Min Shen, Wang Sumin, 2013. Comparison between reconstructions of global anthropogenic land cover change over past two millennia. *Chinese Geographical Science*, 23(2): 131–146. doi: 10.1007/s11769-013-0596-7

1 Introduction

Land use and land cover change (LUCC) which related to human activities and economics closely, plays an important role in global climate change (Turner *et al*., 1993). There are two main parts in LUCC, i.e., the anthropogenic land cover change (ALCC, human-induced land cover change or land use change) and natural land cover change. In the 1990s, the studies on LUCC have been carried out under two international programs, the International Geosphere-Biosphere Programme (IGBP) and the International Human Dimensions Programme on Global Environmental Change (IHDP). Since then, the researches on the causes and effects of the LUCC have

Received date: 2012-04-18; accepted date: 2012-07-19

Foundation item: Under the auspices of Strategic and Special Frontier Project of Science and Technology of Chinese Academy of Sciences (No. XDA05080800), National Basic Research Program of China (No. 2010CB950102), National Natural Science Foundation of China (No. 40871007)

Corresponding author: LIU Jian. E-mail: jianliu@niglas.ac.cn

been done worldwide (Bonan, 1999; Verberg and Van Keulen, 1999; Chen and Verberg, 2000; Chen *et al*., 2000; Houghton, 2003; Wu *et al*., 2003; Foley *et al*., 2005; Zhang and Chen, 2007; Yang *et al*., 2009; Fan *et al*., 2011; Ma *et al*., 2011; Zhu and Chang, 2011). Dirmeyer and Shukla (1994) found that climate change, particularly rainfall, was strongly dependent on the change in surface albedo that accompanied deforestation in the Amazon Basin. Brovkin *et al*. (1999) carried out a set of experiments and found that deforestation caused a global cooling of 0.35℃ with a more notable cooling of 0.5℃ in the Northern Hemisphere. Fu (2003) did a pair of numerical experiments and the results showed that the changes in land cover would bring significant changes to the East Asian monsoon. Li *et al*. (2006) found by a series of modeling experiments that historical LUCC (such as deforestation, degradation of grasslands) had significant impacts on regional climate change. Gao *et al*. (2007) investigated the climate effects of modern land use change over China, and the results showed that the current land use change influenced local climate as simulated by the model through the reinforcement of the monsoon circulation in both the winter and summer seasons and through changes of the surface energy budget. Ge *et al*. (2008) and Kaplan *et al*. (2010) pointed out that the carbon storage and emissions were closely related to the LUCC.

Human activity on land (or ALCC) is one important aspect of anthropogenic climate change. To understand the influence of ALCC on climate, numerical simulation is the most sophisticated tool (Wilson and Henderson-Sellers, 1985). The LUCC/ALCC datasets are then needed as the input data for these climate simulations. After the 1970s, remotely sensed LUCC datasets have been developed with the advent of satellites. They are not only accurate enough for the study of LUCC after the 1970s, but also could be consulted for historical reconstructions. The historical LUCC, especially ALCC, could be reconstructed by collecting sources like national censuses, tax records, forest surveys, paleo records, *etc*., and by developing models. Since the 1980s, a lot of LUCC/ALCC datasets for regional and global coverages have been developed gradually (Iverson, 1988; Loveland *et al*., 2000), along with increased spatial and temporal resolutions. Rosch (1996) introduced the approaches to the land-use reconstruction during Late Neolithic and Bronze Age using botanical on-site and off-site data (including the archaeological sites and pollen sites) in the southwestern Germany. Ramankutty and Foley (1999a) initialized the simulation with a satellite-derived characterization of present-day cropland *c.* 1992, then used it within a simple model, along with historical cropland inventory data at the national and sub-national level, to reconstruct historical crop cover in North America between 1850 and 1992, at a spatial resolution of 5-min. Ramankutty (2004) first established a linear model between the population density dataset and the cropland inventory dataset to simulate a spatially explicit map of croplands for West Africa. Then, he determined the categorical crop-use intensity dataset by calibrating it against the cropland inventory dataset. Finally, he merged these two datasets and adjusted to match the cropland inventory dataset to create a new spatial distribution dataset of croplands for West Africa over the last 50 years. Kaplan *et al*. (2009) created an anthropogenic deforestation for agriculture and pasture (i.e., ALCC) in Europe over the past three millennia by 1) digitizing and synthesizing a dataset of population history for Europe and surrounding areas; 2) developing a model to simulate anthropogenic deforestation based on population density that handles technological progress; and 3) applying the database and model to a gridded dataset of land suitability for agriculture and pasture to simulate spatial and temporal trend in anthropogenic deforestation. He *et al*. (2012) reconstructed the historical cropland area in the Mid-Northern Song Dynasty of China (AD 1004–1085), using the taxes-cropland area and number of families compiled from historical documents. Their estimations were accomplished through analyzing the contemporary policies of tax, population and agricultural development. Then, they converted the political region-based cropland area to geographically explicit grid cell-based fractional cropland, based on calculating cultivation suitability of each grid cell using the topographic slope, altitude and population density as the independent variables. These regional reconstructions were mainly focused on the cropland, i.e., only one part of the ALCC.

The global ALCC has gotten more concerns with an increasing awareness of global scale climate change. The global ALCC datasets which have been used in the simulations include: the distributions of different vegetation types from Olson and Watts (1982), Matthews (1983), Olson *et al*. (1983), and Wilson and Hender-

son-Sellers (1985), the distribution of the vegetation from Olson (1994) as well as DeFries and Townshend (1994), the map of the crop and pasture from Goldewijk *et al*. (1997), the fraction of the crop from Ramankutty and Foley (1998; 1999b, RF dataset hereafter), and the fractions of 18 vegetation types from Leff *et al*. (2004), *etc*. RF dataset has been developed these days and been applied the fractions of the pasture. But so far, the above mentioned climate simulations are mainly restricted to the past 300 years and modern period, the similar climate simulation for the past 2000 years is urgently requested. Because the past two millennia is a critical period for estimating the uncertainties of the anthropogenic climate change, and for understanding the decadal-centennial variability of the Earth system, it has been the core of many global change research programs (e.g., IGBP and World Climate Research Programme (WCRP)), and National Basic Research Program of China, as well as the Strategic and Special Frontier Project of Science and Technology of Chinese Academy of Sciences.

In order to carry out the climate simulation for the past two millennia, to analyze the effect of ALCC on global climate change, the reliable and continuous ALCC datasets for the past two millennia are needed. So far, the most popular and available ALCC datasets covering the past 1000–2000 years include the History Database of the Global Environment (HYDE) (Goldewijk, 2001), Kaplan and Krumhardt (KK) (Kaplan *et al*., 2010) and Pongratz (Pongratz *et al*., 2007) datasets. The datasets of Pongratz and KK have been used in the millennium simulations of the Paleoclimate Modelling Intercomparison Project Phase III (PMIP3) and the Coupled Model Intercomparison Project Phase V (CMIP5). The HYDE dataset has released version 3.1 (Goldewijk *et al*., 2011), which is an updated and internally consistent combination of historical population estimates and also the implementation of improved allocation algorithms with time-dependent weighting maps for cropland and grassland, and the period covered has extended to 10 000 BC to AD 2000. KK dataset has also been developed nowadays. What are the characteristics of these datasets? Are there any differences among them? Which dataset is more realistic, as one of the forcings, for climatic simulation? These questions are being addressed in this paper.

2 Datasets and Methods

Three global datasets of reconstructed ALCC are introduced and compared in this study, in order to find out which one is better as the forcing for climate simulation over the past two millennia.

2.1 KK10 dataset

KK10 dataset is named after the two major investigators, Kaplan and Krumhardt, who made the reconstruction in AD 2010. The dataset provides the fraction of each grid cell that is occupied by anthropogenic land use, i.e., 1 means 100% of the grid cell that is used by people, 0 means the grid cell is occupied by potential natural vegetation.

In order to obtain the reconstruction of ALCC, a common way is to develop a statistical relationship between population and land use. Different relationship models are used in different datasets. Kaplan *et al*. (2009) developed a deforestation model to simulate anthropogenic deforestation based on population density that handled technological progress. The main difference between KK10 and the other datasets is the relationship between population density and land use, which is nonlinear in KK10 but linear in the others. Because the relationship changed after the industrial revolution, and even reversed in some areas, KK10 is more realistic in this regard.

The population database used in KK10 was mainly based on the charts and spot estimates in McEvedy and Jones (1978), supplemented by other information wherever possible (Krumhardt, 2010). Kaplan and his colleagues separated the globe into 12 major groups of population regions, with several sub-regions in each group, and then estimated the population densities and the fractions of croplands and pasture in these sub-regions, which made the estimation more realistic.

Kaplan *et al*. (2009) established the relationship between population and deforestation based on two principles after Mather *et al*. (1998). First, population growth stimulates the expansion of arable land for growing more food, which generally results in deforestation. Second, a growing population means an increased usage of forest products, which can lead to an overall decline of forest area. They normalized both the population density and the forest cover record to eliminate the differences in the proportion of arable land and land productivity among countries. With the development of science and technology, the agricultural products in the same piece of arable land would be available for more people; therefore, deforestation would be reduced, and

some farmlands were returned to forest in some places. Adding the development of science and technology, Kaplan and his colleagues obtained the relationship equation between population and forest, by changing the parameters that represent technological development and intensification in the population-deforestation relationship, and the equation is as follows:

$$FC_{\text{norm}} = \frac{0.9958}{1 + e^{b(c - P_{\text{norm}})}} \quad (1)$$

where FC_{norm} is the normalized forest cover only on usable land, P_{norm} is the normalized population density, and b and c are the parameters representing the technological development and intensification. For different scenarios, Kaplan and his colleagues adjusted the parameters (Table 1).

The land suitability for cultivation (S_{crops}) is calculated as a function of climate and soil variables (Ramankutty *et al*., 2002), and the equation is:

$$S_{\text{crops}} = f(GDD) \times f(\alpha) \times f(pH_{\text{soil}}) \times f(C_{\text{soil}}) \quad (2)$$

where GDD is growing degree days, α is the ratio of actual evapotranspiration (AET) to potential evapotranspiration (PET), C_{soil} is carbon density of soil, and pH_{soil} is pH of soil.

Because plants generally grow everywhere the climate allows, pasture suitability (S_{usable}) is calculated by using only climatic variables, therefore,

$$S_{\text{usable}} = f(GDD) \times f(\alpha) \quad (3)$$

Actually, S_{crops} has been included in S_{usable}, so the result of ($S_{\text{usable}} - S_{\text{crops}}$) is used to calculate the fraction of pasture in one grid cell.

Kaplan *et al*. (2009) first simulated the deforestation over Europe covering 1000 BC to AD 1850 with the above mentioned population, climate and soil database and the deforestation model. Then, they expanded the European ALCC dataset into an annually resolved global ALCC dataset covering the past 8000 years. Because the former dataset was developed using the observations in Europe, and the potential productivity of land for agriculture and pasture was much higher in the tropical regions and lower in boreal regions, they used a high-resolution map of potential Net Primary Productivity (NPP) for the mid-twentieth century produced by a coupled biogeography and biogeochemistry vegetation model (BIOME4, Kaplan, 2001) to rescale ALCC according to the potential productivity of land by using Equation (4):

$$ALCC = ALCC(1.5 - NPP/1400)$$
$$|NPP > 700 \text{ g/(m}^2\cdot\text{yr)}| \quad (4)$$

where NPP is on average roughly twice as high in the most productive areas of the world (~1400 g/(m^2·yr)) as it is in most of Europe (~700 g/(m^2·yr)). To avoid overestimating ALCC in cool-temperate and boreal regions, which are not typically intensively exploited for agriculture in any case, this equation was applied only in areas with NPP exceeding the European average of 700 g/(m^2·yr) (Kaplan, 2001).

2.2 HYDE3.1 dataset

The HYDE database was originally designed for testing and validating the Integrated Model to Assess the Global Environment model (IMAGE 2) (Goldewijk, 2001). The historical cropland and pasture databases were developed by using the historical population estimation as a proxy of agricultural land (including cropland and pasture). Like the KK10 dataset, Goldewijk and his colleagues split the globe into 19 groups, with several sub-regions in each group, then estimated the population density and allocated cropland and pasture in these sub-regions. The HYDE3.1 dataset used here comes from the website (http://themasites.pbl.nl/en/themasites/hyde/download/index. html), with 5-min spatial resolution, the temporal resolutions are as followings: 10 years from AD 1700 to AD 2000, 100 years from AD 1 to AD 1700, and 1000 years before AD 1. The cropland and pasture are defined following the definitions of the Food and Agricultural Organization of the United Nations

Table 1 Values of parameters (b and c) for various curve fits of P_{norm} vs. FC_{norm} described by Eqation (1) in different technological progress

Parameter	Standard scenario	350 BC	AD 1000	AD 1350	AD 1830
b	–3.0	–5.0	–6.0	–7.5	–7.0
c	1.40	0.91	1.36	1.69	1.85

Source: after Kaplan *et al*., 2009

(FAO).

The population database used in HYDE mainly comes from McEvedy and Jones (1978), Livi-Bacci (2007) and Maddison (2001), supplemented with the sub-national population numbers including the population time series at the levels of provinces and states. The spatially explicit distribution was obtained by using weighing maps based on the population density map patterns of Landscan (2006) for current time periods, and gradually replacing them with weighing maps based on proxies, such as distance to water and soil suitability when going back in time (Goldewijk *et al*., 2010). Starting points were the cropland and pasture of whole countries from FAO (2008), which presented data for the post-1961 period based on country scale. Divided by the population of the country, it yielded a per capita use of cropland and pasture. For the pre-1961 period, they assumed that the per capita values for cropland and pasture were not constant, but slightly increase or decrease over time. By estimating the per capita use of cropland and pasture country by country, they then derived the historical pathways of agricultural areas. For a representation of current land cover, the 5-min resolution current global cropland and grassland maps developed by Goldewijk *et al*. (2007) were used. This current land-cover map was used as a weighing map ($W_{\text{crop\_satellite}}$).

The allocation rules for the cropland in HYDE were as follows. First, the grid cells with the highest population density were first assigned to cropland, and then those with the second highest density, until the total amount of cropland was allocated in that unit. Then, the allocation of cropland was restricted to the agricultural area as determined by the initial land cover map. National/sub-national crop area statistics were allocated to grid cells according to a mix of two weighing maps: the above mentioned current map ($W_{\text{crop\_satellite}}$), and a historical one, which was constructed according to the following assumptions. There were six major assumptions when allocating historical cropland: 1) in urban built-up areas (U_{area}), no allocation was allowed; 2) in areas with population density lower than 0.1 person/km^2 (W_{popd}), no allocation was allowed; 3) land with the highest soil suitability for crops was colonized first (W_{suit}); 4) coastal areas and river plains were more favorable for early settlement due to easy accessibility (W_{river}); 5) steep terrain with high slopes was less attractive for settlement and agriculture (W_{slope}); and 6) below the threshold of an mean annual temperature of 0℃ no agricultural activity was assumed ($W_{\text{temp\_crop}}$). The influence of satellite maps increased gradually from 10 000 BC to AD 2000 until the cropland distribution equaled the satellite map distribution. Cropland was allocated by combining historical cropland area statistics with various weighing maps.

(1) Current weighing map for allocation:

$$W_{\text{crop2000}} = W_{\text{satellite2000}} \tag{5}$$

(2) Historical weighing maps:

$$W_{\text{crop},t} = \mathrm{W}_{\text{area},t} \times W_{\text{popd},t} \times W_{\text{suit}} \times W_{\text{river}} \times W_{\text{slope}} \times W_{\text{temp\_crop}} \tag{6}$$

and

$$W_{\text{area},t} = [G_{\text{area},t} - U_{\text{area},t}] / G_{\text{area max}} \tag{7}$$

where, $W_{\text{crop},t}$ is the weighing of the crop area for the tth year; $W_{\text{area},t}$ is the weighing of areas excluding the urban area for the tth year; $W_{\text{popd},t}$ is the weighing of population density for the tth year; $G_{\text{area},t}$ is the total land area (no ice and snow); $U_{\text{area},t}$ is the urban built-up area for the tth year; and $G_{\text{area max}}$ is the maximum area of a 5-min grid cell. Only $W_{\text{area},t}$ and $W_{\text{popd},t}$ changed over time.

There were also two rules for allocating pasture: 1) the total amount of pasture in a country or state was also allocated according to population density, while excluding those grid cells that were already allocated to cropland; and 2) the allocation of pasture was restricted to the agricultural area as determined by the initial land cover map. National/sub-national pasture area statistics were allocated to grid cells according to a mix of two weighing maps: a current one, which was constructed from a satellite map of AD 2000 for pasture (Goldewijk *et al*., 2007), and a historical one, which was constructed according to the following assumptions. Four assumptions were made when allocating the pasture: 1) in urban areas (U_{area}) and areas already occupied by cropland (C_{area}), no allocation was allowed; 2) in areas with population density lower than 0.1 person/km^2 (W_{popd}), no allocation was allowed; 3) natural herbaceous areas as defined by the BIOME model (Prentice *et al*., 1992) were more attractive for use of livestock/pastoral activities (W_{biome}); 4) below the threshold of –10℃ for the annual air temperature no year-round pastoral activity was assumed to happen ($W_{\text{temp\_pasture}}$). The influence of satellite maps increased gradually from

10 000 BC to AD 2000 until the pasture distribution was equal to the satellite map distribution. So,

$$W_{\text{pasture},t} = W_{\text{area},t} \times W_{\text{popd},t} \times W_{\text{biome}} \times W_{\text{temp\_pasture}} \quad (8)$$

$$W_{\text{area},t} = [G_{\text{area},t} - U_{\text{area},t} - C_{\text{area},t}] / G_{\text{area max}} \quad (9)$$

where $C_{\text{area},t}$ is the area occupied by cropland for the tth year.

2.3 Pongratz dataset

The global ALCC dataset provided by Pongratz *et al*. (2007) comes from http://cera-www. dkrz.de/WDCC/ui/Entry.jsp?acronym=RECON_LAND_COVER_800-1992, with annually resolved temporal resolution and 0.5-degree spatial resolution, and it includes 14 vegetation types (Table 2).

Table 2 Vegetation types in Pongratz dataset

Type code	Vegetation
1	Tropical evergreen forest
2	Tropical deciduous forest
3	Temperate evergreen broadleaf forest
4	Temperate/boreal deciduous broadleaf forest
5	Temperate/boreal evergreen conifers
6	Temperate/boreal deciduous conifers
7	Raingreen shrubs
8	Summergreen shrubs
9	C3 natural grasses
10	C4 natural grasses
11	Tundra
12	Crop
13	C_3 pasture
14	C_4 pasture

Pongratz *et al*. (2008) reconstructed the ALCC for AD 1700–1992 and for AD 800–1700 separately. For the reconstruction of crop over the past 300 years (AD 1700–1992), they used the global cropland dataset provided by Ramankutty and Foley (1999b), and made some regional modifications according to the updated data and some historical events. For the reconstruction of pasture over the past 300 years, they extended the pasture map for 1992 provided by the Center for Sustainability and the Global Environment (SAGE) to a time series covering AD 1700–1992, by calculating regional totals of pasture area for each year from the areas and rates of change in AD 1992 from Goldewijk (2001) on country level after 1960, and by adding some regional modifications. For the period of AD 800–1700, they assumed that agriculture occurred wherever people had settled, and the amount of land under human use was likely well correlated to the number of people who had to be nourished. For this reason, they used population estimate as proxy for agricultural area. The main source of population data for AD 800–1700 was the Atlas of World Population History from McEvedy and Jones (1978), with regional modifications for Central and South America, and broke the historical numbers down to country level using the HYDE population density map of AD 1700, assuming that the national proportion within a region remained constant. For some regions, sub-national data was used, especially for the Former Soviet Union and Central and South America. Population numbers were then translated into estimates of crop and pasture area for each country.

2.4 KK10-merged dataset

Kaplan *et al*. (2011) expanded KK10 from AD 1850 to AD 2000 by making a smooth transition between KK10 and HYDE3.1 (Goldewijk *et al*., 2011) during a period that covered AD 1500 to AD 1961. They used exactly the same data as in the HYDE3.1 dataset from AD 1961 to AD 2000 since HYDE3.1 used the FAO crop and pasture statistics, which they considered to be reliable.

For the period from AD 1500 to AD 1961, they first compared the corresponding grid cells between HYDE3.1 and KK10 datasets, and decided the starting point for the data merge at any time between AD 1500 and AD 1850 that the two datasets matched within 1%. If the grid cells matched, they then blended the datasets from the time of the match; if never matched over this period, then they started the blending at AD 1850. In order to capture the variability of HYDE3.1 over the last several centuries, they first calculated the difference between the actual HYDE3.1 ALCC estimates and a direct linear interpolation of the HYDE3.1 data at the starting point of blending (determined as described above) to 1961. Subsequently, this difference was added to a linear interpolation of the KK10 scenario at the starting point of the merge to AD 1961 of HYDE3.1. By doing so, Kaplan and his colleagues created an ALCC dataset that preserves the features of KK10 and covering the whole period of the past two millennia.

In the year of 2011, KK10-merged datasets was updated to KK11-merged dataset, in which the vegetation types required by PMIP3/CMIP5 (same as in Table 2)

were reconstructed. The spatial and the temporal resolutions are the same as those in KK10.

3 Results

3.1 ALCC in typical climatic periods during past 1000 years

Three typical climatic periods during the past 1000 years were chosen according to the simulated time series of the global temperature anomaly over the last millennium (Gao and Liu, 2010). The warmest 100 years of the Medieval Warm Period (MWP) were AD 1100–AD 1199, the coldest 100 years of Little Ice Age (LIA) were AD 1600–AD 1699, and the 90 years of the Present Warm Period (PWP) were AD 1900–AD 1990. Three datasets are compared here, which are HYDE3.1, Pongratz and KK10-merged. The sum of crop, C_3 pasture and C4 pasture in Pongratz and the sum of cropland and pasture in HYDE3.1 dataset are used to compare with the ALCC of KK10-merged dataset. Considering the temporal resolution of HYDE3.1 before AD 1700 was 100 years, the years of AD 1100 and AD 1600 were used to represent MWP and LIA, respectively.

3.1.1 ALCC during Medieval Warm Period

Figure 1 illustrates the fractions of ALCC in the three datasets during the MWP. The fractions of ALCC above 30% in HYDE3.1 only appeared over East Asia (i.e., the lower reaches of the Changjiang (Yangtze) River and the Huanghe (Yellow) River, the West Europe and the Middle East, and some regions over the Caribbean. The fractions of ALCC in Pongratz dataset were the lowest among these three datasets. The fractions were almost under 10% worldwide except over East Asia and England. According to in KK10-merged dataset, much more regions over Europe and Asia had already been occupied by humans during the MWP, especially over West Europe and Indonesia Peninsula. The fractions of ALCC exceeded 60% over West Europe and Indonesia Peninsula and exceeded 40% over East Asia. The three datasets all revealed that the human activities mainly concentrated on the mid-latitude of Eurasia, with the least over the regions of Australia and the Americas.

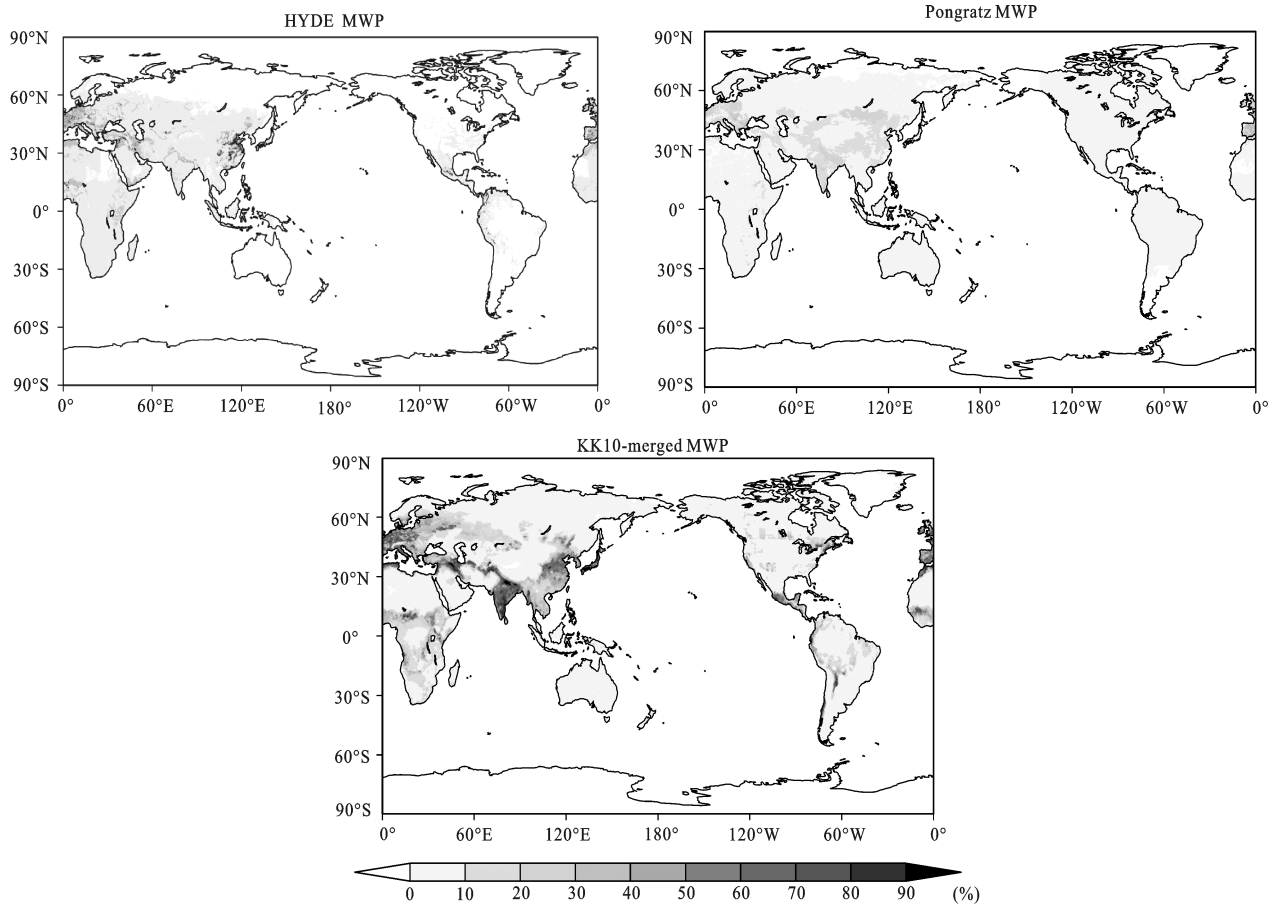

Fig. 1 ALCC fractions from HYDE3.1, Pongratz and KK10-merged datasets during Medieval Warm Period (MWP)

It was warm and wet in the MWP, and the agriculture developed stably, particularly over the regions around the Mediterranean and East Asia. The viticulture developed over the regions of circum-Mediterranean and England during the MWP, which caused increasing cropland. In the regions of East Asia, especially the coastal areas of China in the Song Dynasty, a rapid growth of population led to intensive land use. Meanwhile, because of the lack of technology, more forests were reclaimed to meet the needs of people. This is more accurately reflected in KK10-merged and HYDE3.1 than in Pongratz dataset.

As He *et al*. (2012) reconstructed the grid-cell-based reclamation ratio (RR, reclaimed for cropland) pattern over Eastern China during the Song Dynasty (AD 1077), we used it in this paper for comparison as well. Comparing to the RR (cropland fractions) (Fig. 2), the ALCC fractions in Pongratz dataset (including cropland and pasture) were much lower over the eastern China, which was unreasonable. The ALCC fractions in HYDE3.1 (including cropland and pasture) were close to RR, which indicated the underestimated cropland fractions in HYDE3.1. The ALCC fractions in KK10-merged (including all human activities) were higher than RR, which indicated that the cropland fractions in KK10-merged dataset were closer to RR. In this sense, KK10-merged dataset was more reasonable.

3.1.2 ALCC during Little Ice Age

The three datasets all revealed increasing ALCC fraction over Eurasia and decreasing ALCC fraction over some other regions during the LIA (Fig. 3). The ALCC fractions in HYDE3.1 and KK10-merged datasets showed the decreasing trend over the Americas, while no significant change was found in Pongratz dataset. The ALCC area over the Americas was enlarged during the LIA in HYDE3.1 dataset with decreased fraction strength. The ALCC fractions increased over Eurasia and Africa and decreased over Mongolia in Pongratz dataset. The ALCC fractions in KK10-merged dataset increased visibly over Europe and Africa, but changed little over

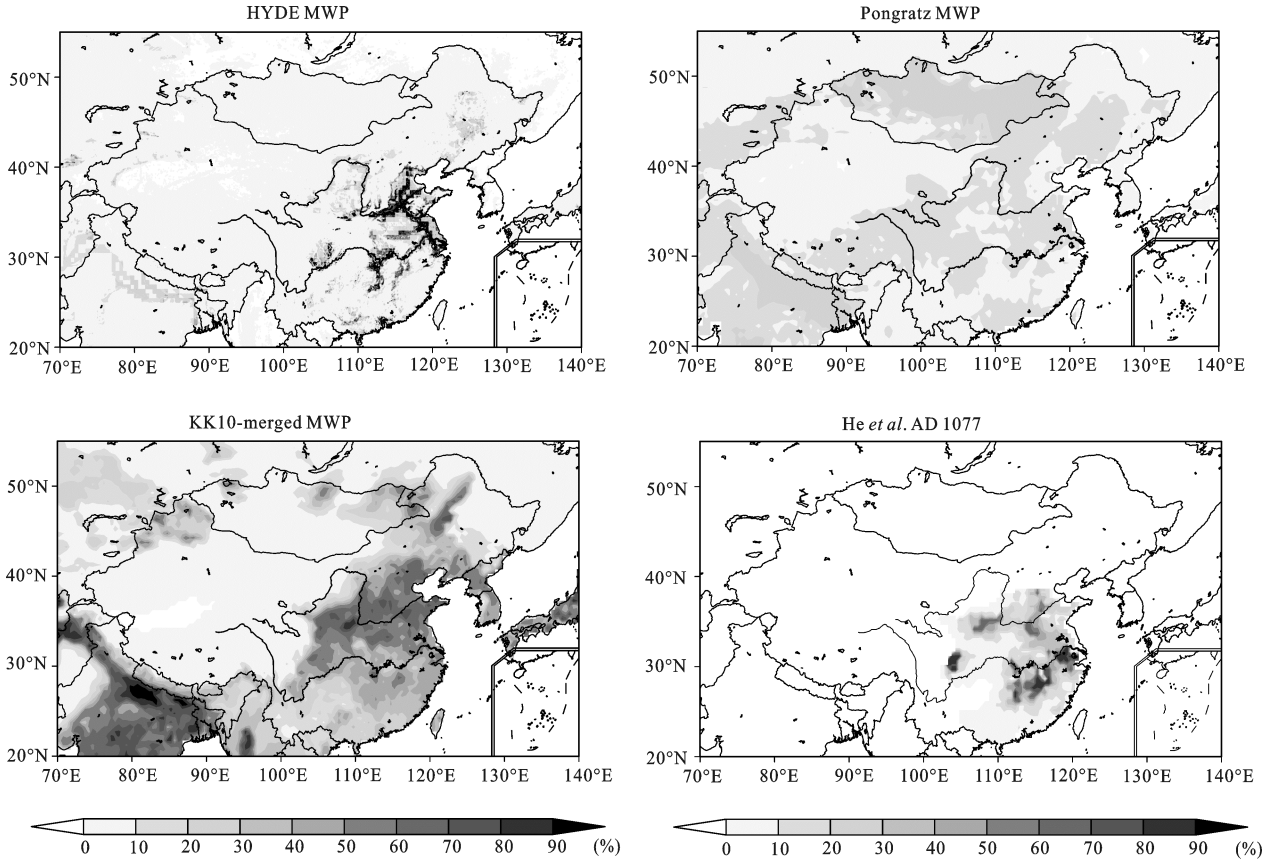

Fig. 2 ALCC fractions over China from HYDE3.1, Pongratz, and KK10-merged datasets during Medieval Warm Period (MWP) (He *et al*. AD 1077 shows reclamation ratio across China, which represents cropland fraction, in the Mid-Northern Song Dynasty reconstructed by He *et al*. (2012))

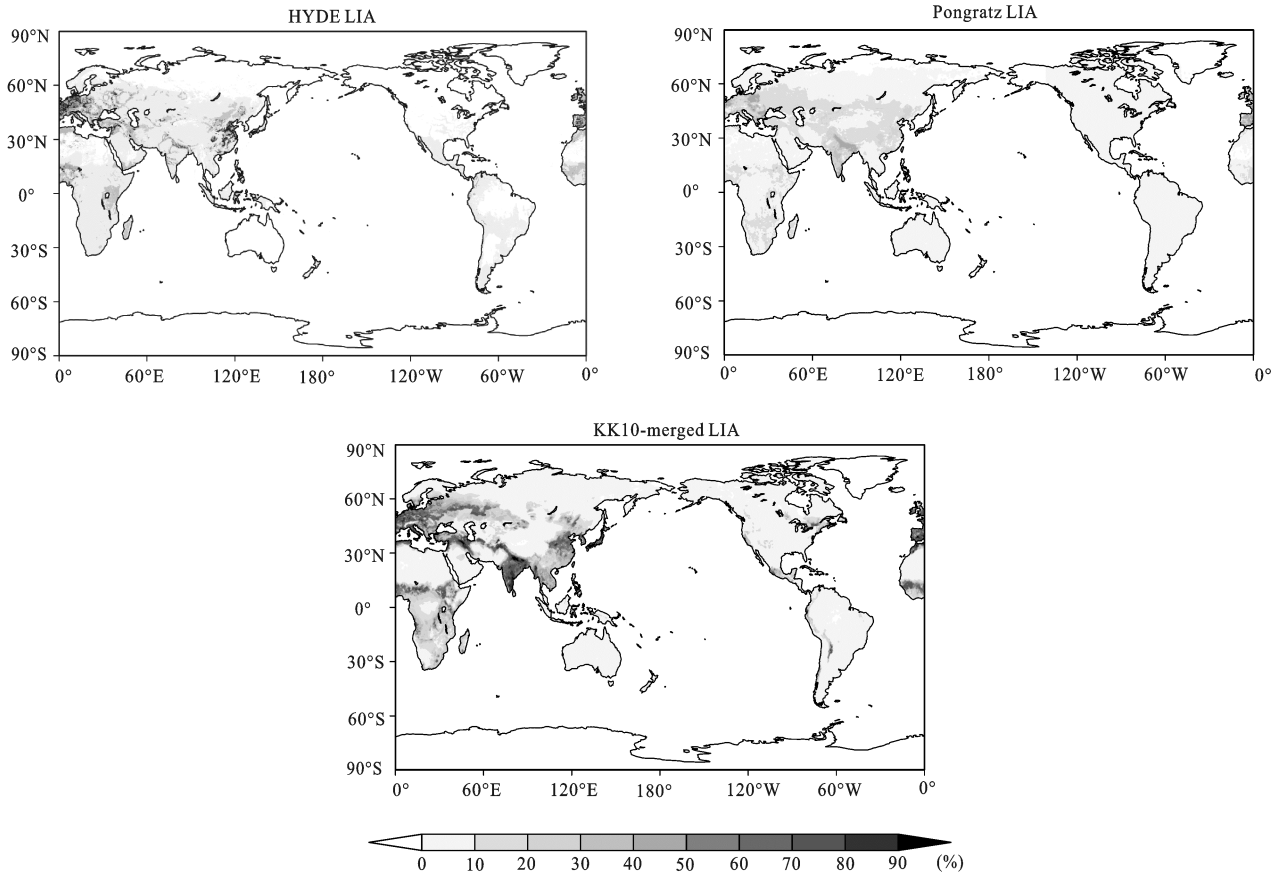

Fig. 3 ALCC fractions from HYDE3.1, Pongratz and KK10-merged datasets during Little Ice Age (LIA)

East Asia, except for the increase over Indochina Peninsula and the decrease over north of the Indochina Peninsula. The ALCC distribution decreased clearly over North America, which might be caused by the reduced colonizing during the LIA.

During the LIA, colder winter occurred in majority of Europe and North America. Farms were destroyed, and the population decreased over the northern regions. In this situation, people had to transform their crops and pastures by changing their species during the 17th and 18th centuries. Therefore, large areas of the Netherlands, England and some other countries around the North Sea were reclaimed (http://www.eh-resources.org/timeline/timeline_lia.html). China was in the Ming and Qing dynasties during the LIA, the population density in the middle reaches of the Changjiang River increased largely because of the migration during the wars, which led to the enlarged area of cropland and higher fractions of ALCC. These are the causes for the increased ALCC fractions in the three datasets. Unfortunately, the fraction changes of ALCC over the Americas are not consistent between HYDE3.1/KK10-merged datasets and Pongratz dataset.

3.1.3 ALCC during Present Warm Period

The ALCC fractions in the three datasets all increased significantly during the Present Warm Period (Fig. 4). The rate of the increase in Pongratz dataset was much higher than that in the other two datasets. The ALCC fractions in Pongratz dataset were higher than 50% over Eurasia and North America, which were higher than those in the other two datasets. The distribution of the fractions in KK10-merged dataset was similar to that in HYDE3.1 but different from that in Pongratz dataset, especially over Australia. The fractions in Pongratz dataset were above 40% over North and East Australia, and were lower than 30% over Central and West Australia, which were almost opposite to those in the other two datasets. The fractions in KK10-merged dataset were lower than those in HYDE3.1 and Pongratz, especially over the Qinghai-Tibet Plateau, which were more reasonable.

The three ALCC datasets during the PWP all re-

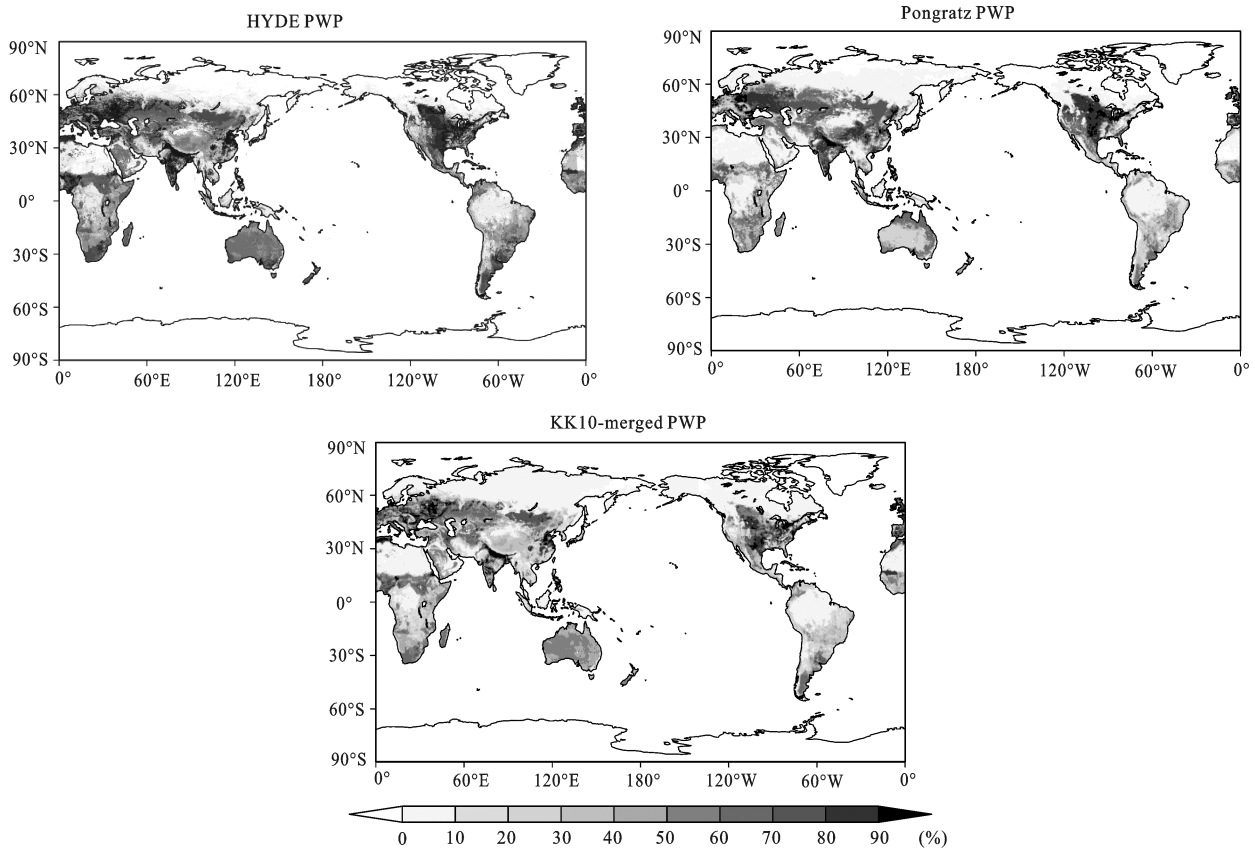

Fig. 4 ALCC fractions from HYDE3.1, Pongratz and KK10-merged datasets during Present Warm Period (PWP)

flected that, with dramatic population increase and the ALCC area enlarged, the potential vegetation was seriously damaged. The difference among these three datasets lied in the fractions over Central Australia and Central Asia (i.e., the western China). The human activities over the Qinghai-Tibet Plateau were overestimated in HYDE3.1 and Pongratz datasets obviously.

3.2 Global ALCC over past two millennia

Since the time series of Pongratz dataset only covers the past 1200 years, the datasets to be compared in this section are the HYDE3.1 and KK10-merged datasets.

Figure 5 shows the global ALCC fractions depicted by the two datasets. The reconstruction of HYDE3.1 showed that the ALCC fractions were only 30%–40% over those regions in the northern Mediterranean and the northeastern China. The ALCC fractions increased over West Europe and East Asia after AD 1000. The ALCC fractions increased over Central America slightly, and increased gradually to 20% over Tropical Africa. The ALCC fractions in AD 1500 decreased compared to those in AD 1300. After AD 1700, with the development of the Industrial Revolution, the ALCC fractions increased rapidly over Eurasia but only slowly over Africa, while they changed little over the Americas. The ALCC fractions over Africa, the Americas and Australia increased significantly only after AD 1950.

The ALCC fractions in KK10-merged dataset had already reached 40% over Eurasia since AD 1. The ALCC fractions increased most significantly over Europe, and changed little over the low latitude of Africa and the other regions during AD 1000–AD 1500. The ALCC fractions decreased significantly during AD 1600 and AD 1700 over the Americas because of the decreasing colonization from Europe, while they increased remarkably after the Industrial Revolution when it was at the end of the LIA and the beginning of the warming.

The two datasets both illustrated that the ALCC fractions would increase with the increase of population, particularly after the Industrial Revolution. The ALCC fractions increased rapidly after AD 1850, and mainly concentrated in Eurasia south of 60°N. The ALCC fractions over the Americas and Africa became more than 50% only after AD 1900. The ALCC fractions in

HYDE3.1 were lower than those in KK10-merged before AD 1961, especially over the eastern China, it was more reliable for KK10-merged dataset. As the dataset of KK10-merged used HYDE3.1 after AD 1961, they are the same for the period of AD 1961–AD 2000.

3.3 Spatial patterns of ALCC over China in typical periods during past two millennia

In order to find how the crop and pasture varied over China in the typical climatic periods during the past two millennia, KK11-merged dataset was used in this paper,

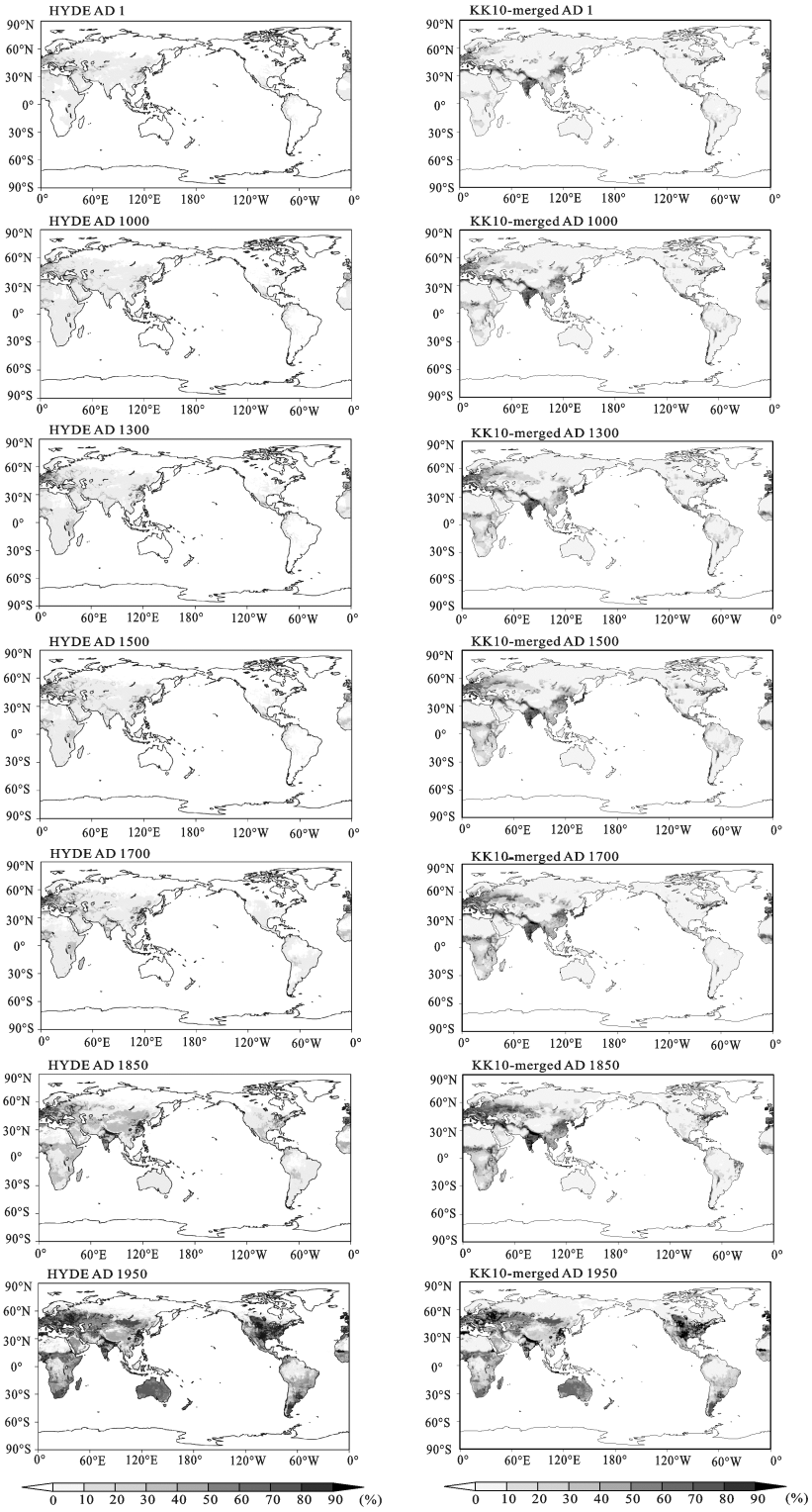

Fig. 5 ALCC fractions from HYDE3.1 and KK10-merged datasets for different timeslices

instead of KK10-merged, since KK11-merged dataset provided the fractions of different vegetation types. Because the temporal resolution of HYDE3.1 was not consecutive, the typical periods for HYDE3.1 were not exactly the same as that for KK11-merged.

The typical climatic periods over China during the past two millennia were confirmed by the winter-half-year mean temperature change during this period in the eastern China, reconstructed by Ge *et al*. (2002). There were totally seven typical periods including the warm periods of the Qin and Han dynasties (AD 100–200), the Sui and Tang dynasties (AD 570–770) and the Song and Yuan dynasties (AD 1201–1290, corresponding to the MWP); cold periods of the Wei and Jin dynasties (AD 210–560), the Five Dynasties (AD 780–920) and the Ming and Qing dynasties (AD 1560–1700, corresponding to the LIA), and of course the PWP (AD 1900–2000).

Figure 6 shows the spatially explicit patterns of the fractions of crop and pasture over China during the above mentioned seven periods. The fractions of the crop and pasture increased distinctively over the middle-lower reaches of the Huanghe River and the Huaihe River Valley during the PWP. It could be found from the differences between each two periods (not shown) that the fractions of crop and pasture over Southeast China decreased during the Wei and Jin dynasties, while they increased over the middle and upper reaches of the Huanghe River and to the west and north of this region. During the warm period of the Sui and Tang dynasties, the fractions of crop and pasture increased over most parts of China, especially over the middle and upper reaches of the Changjiang River, the middle and lower reaches of the Huanghe River and Zhuang Autonomous Region of Guangxi. The difference between the fractions of crop and pasture during the cold period of the Five Dynasties and during the warm period of the Sui and Tang dynasties was inconspicuous, and the fractions even increased over Southeast China despite the cooling. The difference between the situation during the warm period of the Song and Yuan dynasties and that during the cold period of the Five Dynasties was in contrast with the difference between the cold period of the Wei and Jin dynasties and the warm period of the Qin and Han dynasties, the fractions of crop and pasture increased by 10% over Hunan, Guangxi and Liaoning provinces during the warm period of the Song and Yuan dynasties. Comparing to the warm period of the Song and Yuan dynasties, the fractions of the crop and pasture during the cold period of the Ming and Qing dynasties increased by 10% over Heilongjiang and Jilin provinces and the middle reaches of the Changjiang River.

The fractions of the crop and pasture still increased over some parts of China during the cold periods in spite of the cooling, except the cold period of the Wei and Jin dynasties. It might be caused by the frequent wars during the cold periods, and the migration caused the increase of the population over some regions, which could therefore lead to the increase in the fractions of the crop and pasture.

4 Discussion

By comparing to the RR (or ′the fractions of cropland′) over East China during the MWP, it could be found that: 1) the fractions of ALCC in Pongratz (including cropland and pasture) were unreasonable by underestimating obviously; 2) the fractions of ALCC in HYDE3.1 (including cropland and pasture) were close to the RR, which could indicate the fractions of cropland to be underestimated; and 3) the fractions of ALCC in KK10-merged were higher than RR, which could indicate the fraction of cropland to be much closer to the ′real′ situation. Moreover, the ALCC fractions after AD 1850 were overestimated over the Qinghai-Tibet Plateau obviously in Pongratz and HYDE3.1 datasets, while slightly in KK10-merged dataset, which could also illustrate that KK10-merged dataset to be more reliable. Therefore, KK10-merged dataset seemed to be the most reasonable one among these three historical ALCC reconstruction datasets, and it could be used for climatic simulations.

Pongratz and her colleagues focused only on ALCC that permanently changed the type of vegetation, taking into account the permanent expansion and abandonment of cropland and pasture. They did not consider wood harvesting and the long-term fallow area resulted from shifting cultivation, which could make their reconstruction unreasonable. And they assumed that the ratio of agricultural areas per capita did not change prior to AD 1700, which could induce some errors when reconstructing. The uncertainties in the SAGE dataset and the world historical population maps of McEvedy and Jones (1978) (e.g., the uncertainty of population reconstruction and the spatial patterns, the allocation of cropland

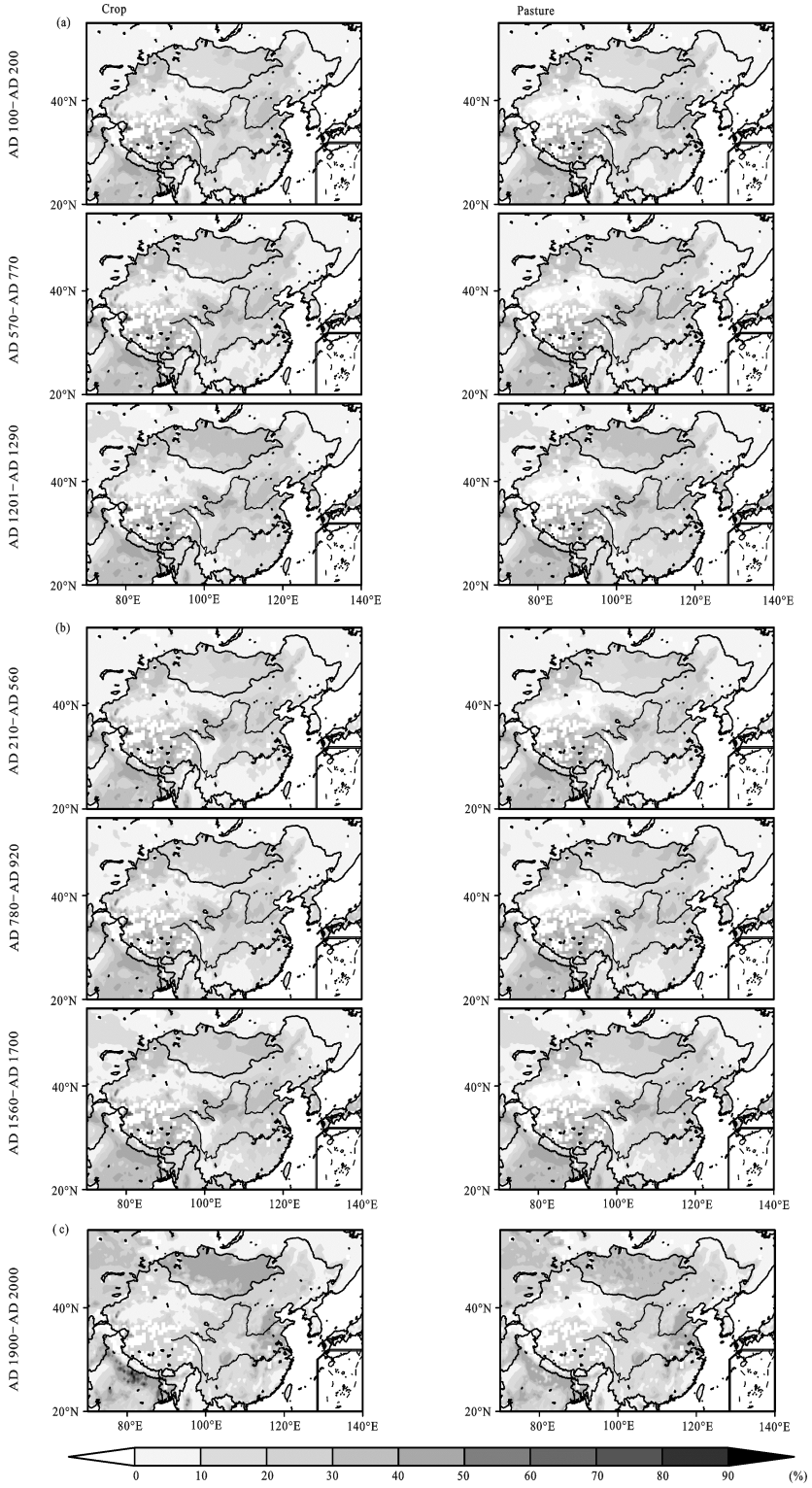

Fig. 6 Spatial patterns of fractions of crop and pasture land over China from KK11-merged dataset in typical climatic periods (a, three warm periods; b, three cold periods; and c, present warm period)

and pasture, *etc*.) also existed in Pongratz dataset. Meanwhile, the Pongratz dataset only covered the period from AD 800 to AD 1992, which could not satisfied the climatic simulation for the past two millennia.

While HYDE3.1 dataset provided high spatial resolution global cropland and pasture over the past 12 000

years, the temporal resolution was coarse and inconsistent (10 years for the period of AD 1700–AD 2000, 100 years for the period of AD 1–AD 1700, and 1000 years before AD 1). Most of all, the relationship between population and land use used in HYDE was a relatively constant relationship similar to the mid-twentieth century. Actually, the relationship before the Industrial Revolution was quite different from that of modern years, which suggested the estimating of HYDE3.1 could have some errors. Secondly, Goldewijk and his colleagues used more weight coefficients when making the reconstruction, which could bring more uncertainties to the reconstruction series.

The historical population density-deforestation relationship used in KK10 and its expanded datasets was nonlinear and Kaplan and his colleagues added the science and technology aspects along with the wood harvesting and the long-term fallow area resulted from shifting cultivation, *etc*. For these reasons, the datasets of KK10 and its expanded ones should demonstrate the characteristics of the historical ALCC more reasonably. Furthermore, to meet the need of climate simulation concerning climatic effects of ALCC, it is necessary to make the continuous distributions of different vegetation types. KK11-merged dataset is the best one for the moment.

Although we choose KK10 and its expanded datasets, there are still some uncertainties lying in the datasets. Some areas (e.g., the Qinghai-Tibet Plateau or Saudi Arabia) have high fractions of ALCC in the form of nomadic pasturing, a low impact, extensive type of land use supporting only small populations of animals and people. On the other hand, Kaplan and his colleagues have noticed that some abandoned land could return back to natural land cover and have considered this situation when reconstructing, but they have not yet considered that some abandoned anthropogenic land cover could not return back to natural land cover. These questions are under consideration by Kaplan and his colleagues.

5 Conclusions

Three reconstructed datasets of global ALCC are compared over the past two millennia in this paper. The KK10 and its expanded datasets are found to be the best for global climate simulation over the past two millennia.

These datasets are not ′data′ in the sense of measured quantities, and they are really just good guesses of what happened and really just ′models′ with many uncertainties (Ramankutty, personal communication). It is better to allocate the potential vegetation by using the population (density) as a proxy. How to estimate the historical population, how to define the potential vegetation, and how to allocate the potential vegetation are the key questions influencing the reconstruction of historical ALCC. For instance, the three datasets all used the population as a proxy, they all based on the world population dataset during 400 BC–AD 1975 provided by McEvedy and Jones (1978), whereas they used different methods to make modifications and to calculate backwards, which resulted in different reconstruction results. How to reduce the uncertainties of the ALCC reconstruction is an issue that needs to be addressed.

References

Bonan G B, 1999. Observational evidence for reduction of daily maximum temperature by croplands in the Midwest United States. *Journal of Climate*, 9(4): 1305–1315.

Brovkin V, Ganopolski A, Claussen M *et al*., 1999. Modelling climate response to historical land cover change. *Global Ecology and Biogeography*, 8(6): 509–517. doi: 10.1046/j.1365-2699.1999.00169.x

Chen Youqi, Verburg P H, 2000. Multi-scale spatial characterization of land use/land cover in China. *Scientia Geographica Sinica*, 20(3): 197–202. (in Chinese)

Chen Youqi, Verburg P H, Xu Bin, 2000. Spatial modeling of land use and its effects in China. *Progress in Geography*, 19(2): 116–127. (in Chinese)

DeFries R S, Townshend J R G, 1994. NDVI-derived land cover classification at a global scale. *International Journal of Remote Sensing*, 15(17): 3567–3586. doi: 10.1080/01431169408954345

Dirmeyer P A, Shukla J, 1994. Albedo as a modulator of climate response to tropical deforestation. *Journal of Geophysical Research*, 99(10): 20863–20877. doi: 10.1029/94JD01311

Fan Yuting, Chen Yaning, Li Weihong *et al*., 2011. Impacts of temperature and precipitation on runoff in the Tarim River during the past 50 years. *Journal of Arid Land*, 3(3): 220–230. doi: 10.3724/SP.J.1227.2011.00220

FAO (Food and Agriculture Organization of the United Nations), 2008. FAOSTAT. Rome, Italy: Food and Agriculture Organization of the United Nations (FAO). Available at: http://www.fao.org (accessed October 2008).

Foley J A, DeFries R, Asner G P *et al*., 2005. Global consequences of land use. *Science*, 309(5734): 570–574. doi: 10.1126/science.1111772

Fu C B, 2003. Potential imapacts of human-induced land cover

change on East Asia monsoon. *Global and Planetary Change*, 37(3–4): 219–229. doi: 10.1016/S0921-8181(02)00207-2

Gao Jian Hui, Liu Jian, 2010. Modeling study on the characteristics and cause of global temperature change during the Last Millennium. *Ludong University Journal* (*Natural Science Edition*), 26(3): 266–270. (in Chinese)

Gao X J, Zhang D F, Chen Z X *et al*., 2007. Land use effects on climate in China as simulated by a regional climate model. *Science in China Series D*: *Earth Science*, 50(4): 620–628. doi: 10.1007/s11430-007-2060-y

Ge Quansheng, Dai Junhu, He Fanneng *et al*., 2008. The land use/land cover change and the carbon emissions over China during the past 300 years. *Science in China Series D*: *Earth Science*, 38(2): 197–210. (in Chinese)

Ge Quansheng, Zheng Jingyun, Man Zhimin *et al*., 2002. Reconstruction and analysis on the series of winter-half-year temperature changes over the past 2000 years in eastern China. *Earth Science Frontiers*, 9(1): 169–181. (in Chinese)

Goldewijk K K, 2001. Estimating global land use change over the past 300 years: The HYDE database. *Global Biogeochemical Cycles*, 15(2): 417–433. doi: 10.1029/1999GB001232

Goldewijk K K, Battjes C G M, Batjes J J, 1997. *A Hundred Year* (*1890–1990*) *Database for Integrated Environmental Assessments. Report 422514002*. Bilthoven, the Netherlands: National Institute for Public Health and the Environment, 188.

Goldewijk K K, Beusen A, Janssen P, 2010. Long term dynamic modeling of global population and built-up area in a spatially explicit way: HYDE 3.1. *The Holocene*, 20(4): 565–573. doi: 10.1177/0959683609356587

Goldewijk K K, Beusen A, Van Drecht G *et al*., 2011. The HYDE 3.1 spatially explicit database of human-induced global land-use change over the past 12000 years. *Global Ecology and Biogeography*, 20(1): 73–86. doi: 10.1111/j.1466-8238.2010.00587.x

Goldewijk K K, Van Drecht G, Bouwman A F, 2007. Mapping contemporary global cropland and grassland distributions on a 5 × 5 minute resolution. *Journal of Land Use Science*, 2(3): 167–190. doi: 10.1080/17474230701622940

He F N, Li S C, Zhang X Z, 2012. Reconstruction of cropland area and spatial distribution in the mid-Northern Song Dynasty (AD 1004–1085). *Journal of Geographical Sciences*, 22(2): 361–372. doi: 10.1007/s11442-012-0932-3

Houghton R A, 2003. Revised estimates of the annual net flux of carbon to the atmosphere from changes in land use and land management 1850–2000. *Tellus Series B-Chemical and Physical Meteorology*, 55(2): 378–390. doi: 10.1034/j.1600-0889.2003.01450.x

Iverson L R, 1988. Land-use changes in Illinois, USA: The influence of landscape attributes on current and historic land use. *Landscape Ecology*, 2(1): 45–61. doi: 10.1007/BF00138907

Kaplan J O, 2001. *Geophysical Applications of Vegetation Modeling*. Department of Ecology, Lund: Lund University, 129.

Kaplan J O, Krumhardt K M, Erle C E *et al*., 2010. Holocene carbon emissions as a result of anthropogenic land cover change. *The Holocene*, 21(5): 775–791. doi: 10.1177/0959683610386983

Kaplan J O, Krumhardt K M, Zimmermann N, 2009. The prehistoric and preindustrial deforestation of Europe. *Quaternary Science Reviews*, 28(27–28): 3016–3034. doi: 10.1016/j.quascirev.2009.09.028

Kaplan J O, Krunmhardt K M, Zimmermann N E, 2011. The effects of land use and climate change on the carbon cycle of Europe over the past 500 years. *Global Change Biology*, 18(3): 902–914. doi: 10.1111/j.1365-2486.2011.02580.x

Krumhardt K M, 2010. ARVE Technical Report#3: *Methodology for World-wide Population Estimates*: *1000 BC to 1850.* Lausanne, Switzerland: école Polytechnique Fédéralede Lausanne, Dept. of Environmental Engineering, ARVE Research Group. Available at: http://arve.epfl.ch/technical_reports/ARVE_ tech_report3_pop_methods.pdf.

Landscan, 2006. *Landscan Global Population Database* (the 2004 revision). Oak Ridge, Tennessee: Oak Ridge National Laboratory. Available at: http://www.ornl.gov/landscan (accessed June 2006).

Leff B, Ramankutty N, Foley J A, 2004. Geographic distribution of major crops across the world. *Global Biogeochemical Cycles*, 18: 27. doi: 10.1029/2003GB002108

Li Qiaoping, Ding Yihui, Dong Wenjie, 2006. A numerical simulation on impact of historical land-use changes on regional climate in China since 1700. *Acta Meterologica Sinica*, 64(3): 257–270. (in Chinese)

Livi-Bacci M, 2007. *A Concise History of World Population* (the 4th edition). Oxford, UK: Blackwell Publishing, 279.

Loveland T R, Reed B C, Brown J F *et al*., 2000. Development of a global land cover characteristics database and IGBP DISCover from 1 km AVHRR data. *International Journal of Remote Sensing*, 21(6–7): 1303–1330. doi: 10.1080/014311600210191

Ma Long, Wu Jinglu, Abuduwaili Jilili, 2011. The climatic and hydrological changes and environmental responses recorded in lake sediments of Xinjiang, China. *Journal of Arid Land*, 3(1): 1–8. doi: 10.3724/SP.J.1227.2011.00001

Maddison A, 2001. *The World Economy*: *A Millennial Perspective*. Paris, France: Organisation for Economic Co-operation and Development/Development Centre (OECD), 384.

Mather A S, Needle C L, Fairbairn J, 1998. The human drivers of global land cover change: The case of forests. *Hydrological Processes*, 12(13–14): 1983–1994. doi: 10.1002/(SICI)1099-1085(19981030)12:13/14<1983::AID-HYP713>3.0.CO;2-M

Matthews E, 1983. Global vegetation and land use: New high resolution data bases for climate studies. *Journal of Climate and Applied Meteorology*, 22(3): 474–487. doi: 10.1175/1520-0450(1983)022<0474:GVALUM>2.0.C0:2

McEvedy C, Jones R, 1978. *Atlas of World Population History.* London: Penguin Books Ltd., 368.

Olson J S, 1994. *Global Ecosystem Framework-definitions*. Sioux Falls, South Dakota: USGS EROS Data Center Internal Report, 37.

Olson J S, Watts J A, Allison L J, 1983. Carbon in live vegetation of major world ecosystems. Oak Ridge, Tennessee: Oak Ridge

National Laboratory, 180.

Olson J, Watts J A, 1982. Major world ecosystem complexes (map, scale 1∶30M). In: Clark W C (ed.). *Carbon Dioxide Review*. Oxford: Oxford University Press, 388–399.

Pongratz J, Reick C, Raddatz T *et al*., 2007. Reconstruction of global land use and land cover AD 800 to 1992. *World Data Center for Climate*. Available at: http://dx.doi.org/DOI:10.1594/WDCC/ RECON_LAND_COVER_800-1992.

Pongratz J, Reick C, Raddatz T *et al*., 2008. A reconstruction of global agricultural areas and land cover for the last millennium. *Global Biogeochemical Cycles*, 22: 16. doi: 10.1029/2007GB003153

Prentice I C, Cramer W, Harrison S P *et al*., 1992. A global biome model based on plant physiology and dominance, soil properties and climate. *Journal of Biogeography*, 19(2): 117–134.

Ramankutty N, Foley J A, 1998. Characterizing patterns of global land use: An analysis of global croplands data. *Global Biogeochemical Cycles*, 12(4): 667–685. doi: 10.1029/98GB02512

Ramankutty N, Foley J A, 1999a. Estimating historical changes in land cover: North American croplands from 1850 to 1992. *Global Ecology Biogeography*, 8(5): 381–396. doi: 10.1046/j.1365-2699.1999.00141.x

Ramankutty N, Foley J A, 1999b. Estimating historical changes in global land cover: Croplands from 1700 to 1992. *Global Biogeochemical Cycles*, 13(4): 997–1027. doi: 10.1029/1999GB900046

Ramankutty N, Foley J A, Norman J *et al*., 2002. The global distribution of cultivable lands: Current patterns and sensitivity to possible climate change. *Global Ecology & Biogeoprophy*, 11(5): 377–392. doi: 10.1046/j.1466-822x.2002.00294.x

Ramankutty, 2004. Croplands in West Africa: A geographically explicit dataset for use in models. *Earth Interactions*, 8(23): 1–22. doi: 10.1175/1087-3562(2004)8<1:CIWAAG>2.0.CO;2

Rosch M, 1996. New approaches to prehistoric land-use reconstruction in southwestern Germany. *Vegetation History and Archaeobotany*, 5(1–2): 65–79. doi: 10.1007/BF00189436

Turner B L, Moss R H, Skole D L, 1993. Relating land use and global land-cover change: A proposal for an IGBP-HDP core project. Stockholm: International Biosphere-Geosphere Program: A study of global change and the human dimensions of global environmental change programme, 65.

Verburg P H, Van Keulen H, 1999. Exploring changes in the spatial distribution of livestock in China. *Agricultural Systems*, 62(1): 51–67. doi: 10.1016/S0308-521X(99)00055-4

Wilson M F, Henderson-Sellers A, 1985. A global archive of land cover and soils data for use in general circulation models. *Journal of Climatology*, 5(2): 119–143. doi: 10.1002/joc.3370050202

Wu H B, Guo Z T, Peng C H, 2003. Land use induced changes of organic carbon storage in soils of China. *Global Change Biology*, 9(3): 305–315. doi: 10.1046/j.1365-2486.2003.00590.x

Yang Xuchao, Zhang Yili, Liu Linshan *et al*., 2009. Sensitivity of surface air temperature change to land types in China. *Science in China Series D*: *Earth Science*, 39(5): 638–646. (in Chinese)

Zhang Jie, Chen Xing, 2007. The historical land use and vegetation cover change in Eastern China. *Journal of Nanjing University* (*Natural Sciences*), 43(5): 544–555. (in Chinese)

Zhu Shujuan, Chang Zhaofeng, 2011. Temperature and precipitation trends in Minqin Desert during the period of 1961–2007. *Journal of Arid Land*, 3(3): 214–219. doi: 10.3724/SP.J.1227.2011.00214